

# Die Swell from Capillary Die and Slit Die: A Theoretical Study

WEN-YEN CHIU and GOANG-DING SHYU, *Department of  
Chemical Engineering, National Taiwan University, Taipei,  
Taiwan, Republic of China*

## Synopsis

Assuming polymer fluids obey the CEF equation, equations concerning die swell from capillary die and slit die were derived. The die swell of polymer increased with increasing shear rate and recoverable shear. Our theoretical predictions conformed well with the experimental data of die swell for PP and PS.

## INTRODUCTION

The die swell of polymer fluid was found to develop by two steps: (1) rapid expansion at the die exit, followed by (2) a further slow expansion. The die swell was defined and measured at some point where the dimension of polymer extrudate no longer changed. At steady state and isothermal condition, several factors affected the die swell of polymers, such as geometry of die, flow rate, temperature, viscoelasticity of polymer, additives, and so on. For examples, Han and Kim<sup>1</sup> studied the effect of aspect ratio of the die ( $L/R$ ) on the die swell of polymer. It decreased with increasing aspect ratio and gradually reached a constant value.<sup>2</sup> As the aspect ratio of die was large enough, the die swell could only be a function of shear rate for the same polymer. Graessley et al.<sup>3</sup> also found an unique relationship between die swell and shear stress under different temperatures. Huang and White<sup>4</sup> investigated the die swell of polymer from both capillary die and slit die. The die swell from slit die was found to be always larger than that from capillary die at the same shear rate for the same polymer. Racin and Bogue<sup>5</sup> found that an increase in molecular weight and molecular weight distribution of polymer shows more significant die swell. Metzner et al.<sup>6</sup> derived an equation relating the die swell and recoverable shear from mass balance and momentum balance. Tanner<sup>7</sup> simulated the polymer fluid as a rubber-like solid and only considered the rapid expansion step in the die swell process. He found that the die swell ( $\chi$ ) could be expressed as a function of recoverable shear ( $S_R$ ) through the following simple equation:  $\chi = (1 + 1/2S_R^2)^{1/6}$ . This equation has been widely used to predict the die swell of polymers. White et al.<sup>4,8-10</sup> derived equations in a similar way for the die swell of polymer from dies with different shapes. Later Tanner et al.<sup>11</sup> and Chang et al.<sup>12</sup> again combined the well known constitutive equation of polymer fluids with the equation of motion and analyzed the die swell phenomena theoretically by using finite-

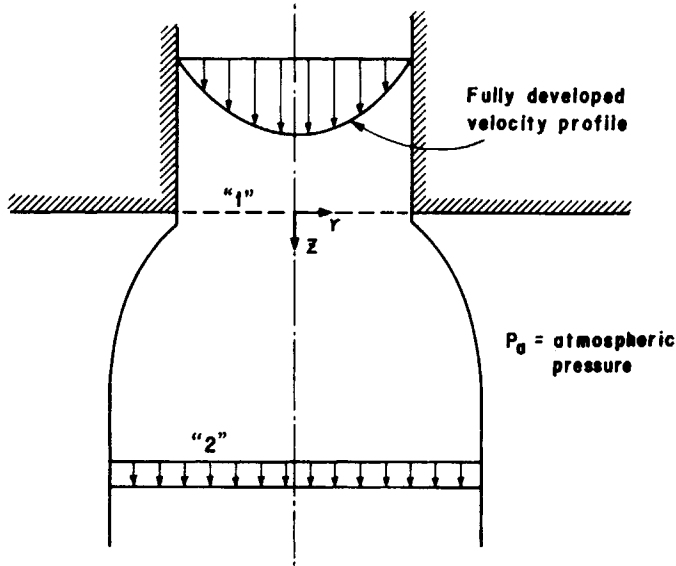


Fig. 1. Velocity profile arrangement in die swell.

element and orthogonal collocation techniques. There were also some empirical equations proposed through dimensional analysis.

In this work, we assumed that polymer fluids obey the (CEF) Criminante-Ericksen-Filbty equation. From mass balance, momentum balance and energy balance, analytic equations were derived to predict the die swell of polymers from either capillary die or slit die, which explained quite well the experimental data done by White et al.<sup>8</sup>

## THEORETICAL TREATMENT

### Die Swell Through Capillary Die

Figure 1 shows the velocity profile arrangement in die swell. Assuming the fluid is incompressible, and the surface tension and gravity are neglected, the mass balance, momentum balance, and energy balance are made between plane 1 and plane 2 of Figure 1.

#### 1. Governing equation

##### (a) Mass balance:

$$\oint \mathbf{n} \cdot \mathbf{v} \, ds = 0 \quad (1)$$

$$\text{i.e.,} \quad \langle v_z \rangle_1 S_1 = v_2 S_2 \quad (2)$$

where  $\langle v_z \rangle_1$ ,  $v_2$ ,  $S_1$ , and  $S_2$  are average velocity at plane 1, uniform velocity at plane 2, cross-sectional area of plane 1, and cross-sectional area of plane 2.

(b) Momentum balance:

$$-\iint(\mathbf{n} \cdot \rho \mathbf{v} \mathbf{v}) \cdot \mathbf{e}_z ds - \iint(\mathbf{n} \cdot \boldsymbol{\pi}) \cdot \mathbf{e}_z ds = 0 \tag{3}$$

After simplification, we get:

$$\rho \langle v_z^2 \rangle_1 - \rho v_2 \frac{S_2}{S_1} + \langle \pi_{zz} \rangle_1 - P_a = 0 \tag{4}$$

where  $\rho$  is the density of fluid,  $P_a$  is atmospheric pressure,  $\boldsymbol{\pi}$  is stress tensor,  $\pi_{zz}$  is  $zz$ -component stress,  $\mathbf{v}$  is the velocity of fluid,  $\mathbf{n}$  is surface normal vector, and  $\langle \rangle_1$  is the average value at plane 1.

(c) Energy balance:

$$-\iint \mathbf{n} \cdot (1/2 \rho \mathbf{v}^2 \mathbf{v}) ds - \iint(\mathbf{n} \cdot \boldsymbol{\pi}) \cdot \mathbf{v} ds + \iiint_{1-2''} (\boldsymbol{\pi} : \nabla \mathbf{v}) dV = 0 \tag{5}$$

which is simplified as:

$$\begin{aligned} & \frac{1}{2} \rho \langle v^2 v_z \rangle_1 S_1 - \frac{1}{2} \rho v_2^3 S_2 + \langle v_r \pi_{zr} \rangle_1 S_1 + \langle v_z \pi_{zz} \rangle_1 S_1 \\ & - P_a v_2 S_2 + \iiint_{1-2''} (\boldsymbol{\tau} : \nabla \mathbf{v}) dV = 0 \end{aligned} \tag{6}$$

where  $\boldsymbol{\tau}$  is dynamic stress tensor,  $\boldsymbol{\pi} = p \boldsymbol{\delta} + \boldsymbol{\tau}$ ,  $\boldsymbol{\delta}$  is unit tensor, and  $v_r$  is  $r$  component velocity.

Assuming the flow of fluid at plane 1 is fully developed. (i.e.,  $v_r = 0$ ). From Eqs. (2), (4), and (6), we obtain:

$$\begin{aligned} & 2\alpha \frac{\langle v_z^2 \rangle_1}{\langle v_z \rangle_1^2} - \frac{\langle v_z^3 \rangle_1}{\langle v_z \rangle_1^3} - 2\alpha \frac{S_1}{S_2} + \left( \frac{S_1}{S_2} \right)^2 - \frac{\alpha \langle \psi_1 \dot{\gamma}^2 \rangle_1}{\frac{1}{2} \rho \langle v_z \rangle_1^2} + \frac{\langle \psi_1 \dot{\gamma}^2 v_z \rangle_1}{\frac{1}{2} \rho \langle v_z \rangle_1^3} \\ & - P_a \frac{(\alpha - 1)}{\frac{1}{2} \rho \langle v_z \rangle_1^2} - \frac{\iiint_{1-2''} (\boldsymbol{\tau} : \nabla \mathbf{v}) dV}{\frac{1}{2} \rho \langle v_z \rangle_1^3 S_1} = 0 \end{aligned} \tag{7}$$

where 
$$\alpha = \frac{\langle \pi_{rr} v_z \rangle_1}{\langle \pi_{rr} \rangle_1 \langle v_z \rangle_1}, \tag{8}$$

$\psi_1$  is primary normal stress coefficient,  $\dot{\gamma}$  is shear rate, and  $\pi_{rr}$  is  $rr$  component stress.

From equation of motion, we can prove that  $\alpha = 1$  as  $\psi_2 = 0$ , where  $\psi_2$  is secondary normal stress coefficient.

## 2. Constitutive equation

Assume that the fluids obey the Criminate-Ericksen-Filbty (CEF) equation, that is:

$$\tau = -\eta \dot{\mathbf{r}} - \left\{ \frac{1}{2} \psi_1 + \psi_2 \right\} \dot{\mathbf{r}}^2 + \frac{1}{2} \psi_1 \frac{\mathcal{D} \dot{\mathbf{r}}}{\mathcal{D} t} \quad (9)$$

where  $\frac{\mathcal{D}}{\mathcal{D} t}$  is corotational derivative, that is,

$$\frac{\mathcal{D}}{\mathcal{D} t} \dot{\mathbf{r}} = \frac{\partial}{\partial t} \dot{\mathbf{r}} + \mathbf{v} \cdot \nabla \dot{\mathbf{r}} + \frac{1}{2} (\mathbf{W} \cdot \dot{\mathbf{r}} - \mathbf{W}) \quad (10)$$

$\dot{\mathbf{r}}$  is rate of strain tensor, and  $\mathbf{W}$  is vorticity tensor. Since  $\psi_2$  is much smaller than  $\psi_1$ , then

$$\tau = -\eta \dot{\mathbf{r}} + \frac{1}{2} \psi_1 \left( -\dot{\mathbf{r}}^2 + \frac{\mathcal{D}}{\mathcal{D} t} \dot{\mathbf{r}} \right) \quad (11)$$

$\eta$  and  $\psi_1$  are functions of the secondary invariant of the rate of strain tensor (i.e.,  $\text{II} \dot{\mathbf{r}}$ ), and can be expressed as follows according to the power law:

$$\eta = \eta_o \left( \frac{1}{2} \text{II} \dot{\mathbf{r}} \right)^{n-1/2} \quad (12)$$

$$\psi_1 = \psi_o \left( \frac{1}{2} \text{II} \dot{\mathbf{r}} \right)^{m-1/2} \quad (13)$$

$$\begin{aligned} \text{II} \dot{\mathbf{r}} &= \dot{\mathbf{r}} : \dot{\mathbf{r}} \\ &= \sum_i \sum_j \dot{r}_{ij} \dot{r}_{ij} \end{aligned} \quad (14)$$

where  $n$ ,  $m$ ,  $\eta_o$ , and  $\psi_o$  are constants.

3. Evaluation of  $\chi$  and  $\langle \rangle_1$  in Eq. (7)

At and prior to plane 1,  $\mathbf{v} = (0, 0, v_z(r))$

$$\begin{aligned} \text{then} \quad \dot{\mathbf{r}} &= \dot{r} \begin{pmatrix} 0 & 0 & 1 \\ 0 & 0 & 0 \\ 1 & 0 & 0 \end{pmatrix}, & \frac{\mathcal{D}}{\mathcal{D} t} \dot{\mathbf{r}} &= \dot{r}^2 \begin{pmatrix} 1 & 0 & 0 \\ 0 & 0 & 0 \\ 0 & 0 & -1 \end{pmatrix}, \\ \dot{\mathbf{r}}^2 &= \dot{r}^2 \begin{pmatrix} 1 & 0 & 0 \\ 0 & 0 & 0 \\ 0 & 0 & 1 \end{pmatrix}, & \tau &= \begin{pmatrix} 0 & 0 & -\eta \dot{r} \\ 0 & 0 & 0 \\ -\eta \dot{r} & 0 & -\psi \dot{r}^2 \end{pmatrix} \\ \psi_2 &= 0 \quad \alpha = 1 \end{aligned} \quad (15)$$

From equation of motion, we obtain:

$$v_z = \left[ \frac{1}{2\eta_o} \left( -\frac{\partial P}{\partial z} \right) \right]^{1/n} \frac{n}{n+1} R_1^{1+1/n} \left[ 1 - \left( \frac{r}{R_1} \right)^{1+1/n} \right] \tag{16}$$

$$\langle v_z \rangle_1 = v_1 = \frac{n}{3n+1} \left[ \frac{1}{2\eta_o} \left( -\frac{\partial P}{\partial z} \right) \right]^{1/n} R_1^{1+1/n}$$

$$\langle v_z^2 \rangle_1 = \frac{3n+1}{2n+1} v_1^2 \tag{17}$$

$$\langle v_z^3 \rangle_1 = \frac{3(n+1)^2}{(2n+1)(5n+3)} v_1^3 \tag{18}$$

$$\langle \psi_1 \dot{r}^2 \rangle_1 = \frac{2n}{m+2n+1} \frac{\left( \frac{3n+1}{n} \right)^{m+1} \psi_o v_1^{1+m}}{R_1^{m+1}} \tag{19}$$

$$\begin{aligned} \langle \psi_1 \dot{r}^2 v_z \rangle_1 &= \frac{2n^2}{(m+2n+1)(3n+m+2)} \left( \frac{3n+1}{n} \right)^{m+2} \psi_o \\ &\times \frac{v_1^{m+2}}{R_1^{m+1}} \end{aligned} \tag{20}$$

$$\frac{S_1}{S_2} = \left( \frac{R_1}{R_2} \right)^2 = \frac{1}{\chi^2} \tag{21}$$

$\chi$  = die swell ratio

$$\dot{r}_w = \frac{3n+1}{n} \frac{v_1}{R_1} \tag{22}$$

Substituting Eqs. (15) ~ (21) into Eq. (7), we get:

$$\begin{aligned} &\frac{(n+3)(3n+1)}{(2n+1)(5n+3)} - \frac{2}{\chi^2} + \frac{1}{\chi^4} \\ &= \frac{4n(m+1)}{(m+2n+1)(3n+m+2)} \left( \frac{3n+1}{n} \right)^{m+1} \\ &\times \frac{\psi_o v_1^{m-1}}{\rho R_1^{1+m}} + \frac{\iiint_{1-2} (\tau : \nabla v) dV}{1/2 \rho v_1^3 S_1} \end{aligned} \tag{23}$$

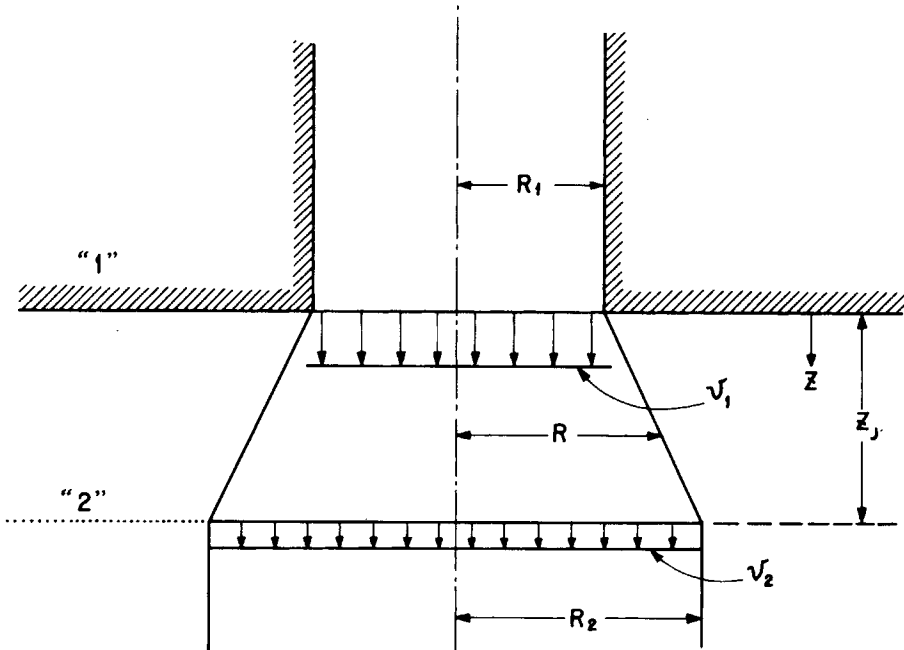


Fig. 2. Crude velocity pattern and extrudate shape for calculation.

#### 4. Evaluation of $(\tau : \nabla v)$

As shown in Fig. 2, the velocity pattern and extrudate shape after die exit are approximated.  $Z_j$  is the required length to attain the steady die swell. Between plane 1 and plane 2,  $v = (v_r, 0, v_z(z))$ , then from mass balance:

$$v_1 R_1^2 = v_2 R^2$$

or

$$v_z = v_1 \left( \frac{R_1}{R_2} \right)^2 = \frac{v_1}{\left( 1 + \frac{\chi - 1}{Z_j} Z \right)^2} = \frac{v_1}{(1 + KZ)^2} \quad (24)$$

$$K = \frac{\chi - 1}{Z_j}$$

Again from equation of continuity, we get:

$$v_r = \frac{K v_1 r}{(1 + KZ)^3} \quad (25)$$

and  $\dot{\mathbf{r}} = \begin{pmatrix} 2\frac{\partial v_r}{\partial r} & 0 & \frac{\partial v_r}{\partial Z} \\ 0 & 2\frac{\partial v_r}{\partial r} & 0 \\ \frac{\partial v_r}{\partial Z} & 0 & 2\frac{\partial v_r}{\partial Z} \end{pmatrix}$  (26)

$$\dot{\mathbf{r}}^2 = \begin{pmatrix} 4\left(\frac{\partial v_r}{\partial r}\right)^2 & 0 & -2\frac{\partial v_r}{\partial Z}\frac{\partial v_r}{\partial r} \\ 0 & 4\left(\frac{\partial v_r}{\partial r}\right)^2 & 0 \\ -2\frac{\partial v_r}{\partial Z}\frac{\partial v_r}{\partial r} & 0 & 4\left(\frac{\partial v_r}{\partial Z}\right)^2 + \left(\frac{\partial v_r}{\partial Z}\right)^2 \end{pmatrix}$$
 (27)

$$\frac{\mathcal{D}}{\mathcal{D}t}\dot{\mathbf{r}} = \begin{pmatrix} -\left(\frac{\partial v_r}{\partial Z}\right)^2 + 2v_z\frac{\partial^2 v_r}{\partial r\partial Z} & 0 \\ 0 & 2v_z\frac{\partial^2 v_r}{\partial r\partial Z} \\ \frac{\partial v_r}{\partial Z}\left(\frac{\partial v_r}{\partial r} - \frac{\partial v_z}{\partial Z}\right) + v_r\frac{\partial^2 v_r}{\partial r\partial Z} + v_z\frac{\partial^2 v_r}{\partial Z^2} & 0 \\ \frac{\partial v_r}{\partial Z}\left(\frac{\partial v_r}{\partial r} - \frac{\partial v_z}{\partial Z}\right) + v_r\frac{\partial^2 v_r}{\partial r\partial Z} + v_z\frac{\partial^2 v_r}{\partial Z^2} & 0 \\ 0 & \\ \left(\frac{\partial v_r}{\partial Z}\right)^2 + 2v_z\left(\frac{\partial^2 v_z}{\partial Z^2}\right) & \end{pmatrix}$$
 (28)

Substituting Eqs. (25) ~ (28) into Eq. (11), we obtain:

$$\tau_{rr} = -\frac{2\eta K v_1}{(1 + KZ)^3} - \psi_1 \left[ \frac{5K^2 v_1^2}{(1 + KZ)^6} + \frac{9K^4 v_1^2 r^2}{(1 + KZ)^8} \right]$$
 (29)

$$\tau_{r\theta} = \tau_{\theta r} = \tau_{\theta z} = \tau_{z\theta} = 0$$
 (30)

$$\tau_{\theta\theta} = -\frac{2\eta K v_1}{(1 + KZ)^3} - \frac{5\psi_1 K^2 v_1^2}{(1 + KZ)^6}$$
 (31)

$$\tau_{zr} = \tau_{rz} = \frac{3\eta K^2 v_1 r}{(1 + KZ)^4} - \frac{3\psi_1 K^3 v_1^2 r}{(1 + KZ)^7}$$
 (32)

$$\tau_{zz} = 4\eta \frac{K v_1}{(1 + KZ)^3} - \frac{2\psi_1 K^2 v_1^2}{(1 + KZ)^6}$$
 (33)

$$\Pi \dot{r} = \frac{6K^2 v_1^2}{(1 + KZ)^6} \left[ 4 + \frac{3K^2 r^2}{(1 + KZ)^2} \right] \tag{34}$$

$$\begin{aligned} \therefore \tau : \nabla \mathbf{v} &= \eta_o \left\{ \frac{3K^2 v_1^2}{(1 + KZ)^6} \left[ 4 + \frac{3K^2 r^2}{(1 + KZ)^2} \right] \right\}^{n-1/2} \\ &\times \left[ -\frac{12K^2 v_1^2}{(1 + KZ)^6} - \frac{9K^4 v_1^2 r^2}{(1 - KZ)^8} \right] \\ &+ \psi_o \left\{ \frac{3K^2 v_1^2}{(1 + KZ)^6} \left[ 4 + \frac{3K^2 r^2}{(1 + KZ)^2} \right] \right\}^{m-1/2} \left[ -\frac{6K^3 v_1^3}{(1 + KZ)^9} \right] \end{aligned} \tag{35}$$

$$\begin{aligned} \frac{1}{S} \iiint_{1-2} (\tau : \nabla \mathbf{v}) dV &= -\frac{\eta_o v_1^{n+1}}{R_1^n} \left\{ \frac{8}{9n(n+1)} (C^{n+1/2} - 12^{n+1/2}) \right. \\ &\times \left( 1 - \frac{1}{\chi^{3n}} \right) \left( \frac{\chi - 1}{J} \right)^{n-2} \\ &+ \frac{2C^{n+1/2}}{3n(n+1)} \left( 1 - \frac{1}{\chi^{3n}} \right) \\ &\times \left( \frac{\chi - 1}{J} \right)^n \\ &\left. - \frac{4(C^{n+3/2} - 12^{n+3/2})}{27n(n+1)(n+3)} \left( 1 - \frac{1}{\chi^{3n}} \right) \left( \frac{\chi - 1}{J} \right)^{n-2} \right\} \\ &+ \frac{\psi_o v_1^{m+1}}{R_1^{m+1}} \frac{4(C^{m+1/2} - 12^{m+1/2})}{9(m+1)^2} \\ &\times \left( 1 - \frac{1}{\chi^{3(m+1)}} \right) \left( \frac{\chi - 1}{J} \right)^{m-1} \end{aligned} \tag{36}$$

where  $C = 12 + 9 \left( \frac{\chi - 1}{J} \right)^2$  (37)

$$J = \frac{Z_J}{R_1} \tag{38}$$

Substituting Eq. (36) into Eq. (23), and multiplying  $\frac{R_1^n \rho v_1^{2-n}}{\eta_o}$  in both sides of



equation, we obtain:

$$\begin{aligned} & \frac{1}{2} \left( 3 + \frac{1}{n} \right)^m R_e \left\{ \frac{(n+3)(3n+1)}{(2n+1)(5n+3)} - \frac{2}{\chi^2} + \frac{1}{\chi^4} \right\} \\ &= S_R \left\{ \frac{4n(m+1)}{(m+2n+1)(3n+m+2)} \left( \frac{3n+1}{n} \right)^{m+1} \right. \\ & \quad \left. - \frac{8}{9(m+1)^2} \left( \frac{\chi-1}{J} \right)^{m-1} \left( 1 - \frac{1}{\chi^{3(m+1)}} \right) (C^{m+1/2} - 12^{m+1/2}) \right\} \\ & \quad - \frac{4}{27n(n+1)} \left( 1 - \frac{1}{\chi^{3n}} \right) \left( 3 + \frac{1}{n} \right)^{1+m-n} \left( \frac{\chi-1}{J} \right)^{n-2} \\ & \quad \times \left\{ 9 \left( \frac{\chi-1}{J} \right) C^{n+1/2} - \frac{2}{n+3} (C^{n+3/2} - 12^{n+3/2}) \right. \\ & \quad \left. + 12(C^{n+1/2} - 12^{n+1/2}) \right\} \end{aligned} \tag{39}$$

where

$$R_e = \frac{2R_1^n \rho v_1^{2-n}}{\eta_o} \left( 3 + \frac{1}{n} \right)^{1-n} \tag{40}$$

$$S_R = \frac{\psi_1}{\eta} \dot{\gamma}_w = \frac{\psi_o}{\eta_o} \dot{\gamma}_w^{1+m-n} \tag{41}$$

In general,  $R_e \ll 1$  for polymer fluids and  $J \sim 1$ , then Eq. (39) becomes:

$$\begin{aligned} & S_R \left\{ \frac{4n(m+1)}{(m+2n+1)(3n+m+2)} \left( 3 + \frac{1}{n} \right)^{m+1} - \frac{8}{9(m+1)^2} \right. \\ & \quad \left. \times (\chi-1)^{m-1} \left( 1 - \frac{1}{\chi^{3(m+1)}} \right) (C^{m+1/2} - 12^{m+1/2}) \right\} \\ &= \frac{4}{27n(n+1)} \left( 3 + \frac{1}{n} \right)^{1+m-n} \left( 1 - \frac{1}{\chi^{3n}} \right) (\chi-1)^{n-2} \\ & \quad \times \left\{ 9(\chi-1)^2 C^{n+1/2} - \frac{2}{n+3} (C^{n+3/2} - 12^{n+3/2}) \right. \\ & \quad \left. + 12(C^{n+1/2} - 12^{n+1/2}) \right\} \end{aligned} \tag{42}$$

Equation (42) shows the relation between die swell ratio ( $\chi$ ) and recoverable shear ( $S_R$ ) for polymer fluids from capillary die.



Fig. 3. Die swell from a slit die.

### Die Swell Through Slit Die

The die swell of polymers from a slit die is roughly shown in Figure 3. Since the ratio of width to thickness of the slit die is much larger than 1, we can neglect the dimension variation of extrudate in the width ( $z$ ) direction, then the velocity of extrudate can be expressed as:  $v = (v_x, v_y, 0)$ .

From mass balance, momentum balance, and energy balance between plane 1 and plane 2, we derive the following equation in a similar way as in capillary die:

$$\frac{\langle v_x^3 \rangle_1}{\langle v_x \rangle_1^3} - 2\alpha \frac{\langle v_x^2 \rangle_1}{\langle v_x \rangle_1^2} + 2\alpha \frac{S_1}{S_2} - \frac{S_1^2}{S_2^2} + \frac{P_a(\alpha - 1)}{\frac{1}{2}\rho \langle v_x \rangle_1^2} + \alpha \frac{\langle \psi_1 \dot{\gamma}^2 \rangle}{\frac{1}{2}\rho \langle v_x \rangle_1^2} - \frac{\langle \psi_1 \dot{\gamma} v_x \rangle_1}{\frac{1}{2}\rho \langle v_x \rangle_1^3} + \frac{\iiint_{1-2} (\tau : \nabla v) dV}{\frac{1}{2}\rho \langle v_x \rangle_1^3 S_1} = 0 \quad (43)$$

where  $S_1$  and  $S_2$  are cross-sectional areas of plane 1 and plane 2 per unit width,

$$\alpha = \frac{\langle v_x \pi_{yy} \rangle_1}{\langle v_x \rangle_1 \langle \pi_{yy} \rangle_1} \quad (44)$$

and  $\pi_{yy}$  is  $yy$  component stress.

At plane 1, the flow of fluid is fully developed,  $v = (v_x(y), 0, 0)$ . Then from equation of motion, we obtain:

$$\tau = \begin{pmatrix} -\psi_1 \dot{\gamma}^2 & -\eta \dot{\gamma} & 0 \\ -\eta \dot{\gamma} & 0 & 0 \\ 0 & 0 & 0 \end{pmatrix}$$

$$\langle v_x \rangle_1 = v_1$$

$$\langle v_x^2 \rangle_1 = \frac{2(2n+1)}{(3n+2)} v_1^2$$

$$\langle v_x^3 \rangle_1 = \frac{6(2n+1)^2}{(3n+1)(4n+3)} v_1^3$$

$$\langle \psi_1 \dot{\gamma}^2 \rangle_1 = \frac{n}{1+m+n} \left( \frac{2n+1}{n} \frac{v_1}{h} \right)^{m+1} \psi_0$$

$$\langle \psi_1 \dot{\gamma}^2 v_x \rangle_1 = v_1 \psi_0 \frac{n(2n+1)}{(n+m+1)(2n+m+2)} \left( \frac{2n+1}{n} \frac{v_1}{h} \right)^{m+1}$$
(45)

Substituting Eq. (45) into Eq. (43), we get:

$$\begin{aligned} & \frac{6(2n+1)^2}{(3n+2)(4n+3)} - \frac{4(2n+1)}{(3n+2)} + \frac{2}{\chi} - \frac{1}{\chi^2} + \frac{n}{1+m+2} \\ & \times \left( \frac{2n+1}{n} \frac{v_1}{h} \right)^{m+1} \frac{\psi_o}{\frac{1}{2}\rho v_1^2} - \frac{n(2n+1)}{(n+m+1)(2n+m+2)} \\ & \left( \frac{(2n+1)}{n} \frac{v_1}{h} \right)^{m+1} \frac{\psi_o}{\frac{1}{2}\rho v_1^2} + \frac{\iiint_{1-2} \tau : \nabla v dV}{\frac{1}{2}\rho v_1^3 S_1} = 0 \end{aligned} \tag{46}$$

where  $\chi = H/h = S_2/S_1 =$  die swell ratio.

The velocity pattern and extrudate shape after die exit are approximated as in Figure 4, then

$$v_x = \frac{v_1}{1 + \frac{H-h}{Z_x}x} = \frac{v_1}{1+kx}$$

Again from equation of continuity:

$$\begin{aligned} v_r &= \frac{kv_1 y}{(1+kx)^2} \\ \dot{\mathbf{r}} &= \frac{2v_1 k}{(1+kx)^2} \begin{pmatrix} -1 & \frac{-ky}{(1+kx)} & 0 \\ \frac{-ky}{(1+kx)} & 1 & 0 \\ 0 & 0 & 0 \end{pmatrix} \\ \boldsymbol{\tau} &= \begin{pmatrix} \frac{2\eta v_1 k}{(1+kx)^2} & \frac{2\eta v_1 k^2 y}{(1+kx)^3} & 0 \\ \frac{2\eta v_1 k^2 y}{(1+kx)^3} & \frac{-2\eta v_1 k}{(1+kx)^2} - \frac{4\psi_1 v_1^2 k^2}{(1+kx)^4} & 0 \\ 0 & \times \left[ 1 + \frac{k^2 y^2}{(1+kx)^2} \right] & 0 \end{pmatrix} \\ \iiint_{1-2} (\boldsymbol{\tau} : \nabla v) dV &= \frac{\eta_o h v_1}{n} \left( 2 \frac{\chi-1}{Jh} v_1 \right)^n \left[ \frac{1}{\chi^{2n}} - 1 \right] \\ \int_0^1 \left[ 1 + \left( \frac{\chi-1}{J} \right)^2 \lambda^2 \right]^{m+1/2} d\lambda &+ \frac{\psi_o v_1 h}{(2m-1)} \left[ 2 \left( \frac{\chi-1}{Jh} \right) v_1 \right]^{m+1} \\ \left[ \frac{1}{\chi^{2m-1}} - 1 \right] \int_0^1 \left[ 1 + \left( \frac{\chi-1}{J} \right)^2 \lambda^2 \right]^{m+1/2} d\lambda & \end{aligned} \tag{47}$$

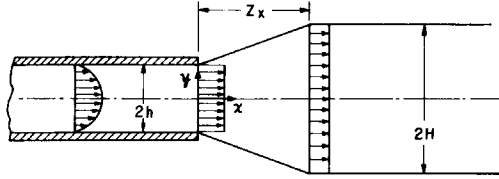


Fig. 4. Crude velocity pattern and extrudate shape for calculation.

where  $J = Z_x/h$ . Substituting Eq. (47) into Eq. (46), we derive the following equation relating the die swell with the recoverable shear for polymer fluids from slit die:

$$\begin{aligned}
 R_e & \left[ \frac{4(n+1)}{3n+2} - \frac{6(2n+1)^2}{(3n+2)(4n+3)} + \frac{1}{\chi^2} - \frac{2}{\chi} \right] \\
 & = 2S_R \frac{(m+1)(2n+1)}{(1+m+n)(2+m+2n)} - 2 \left( 1 - \frac{1}{\chi^{2n}} \right) \left( \frac{2(\chi-1)}{J} \right)^n \\
 & \quad \times \left( \frac{n}{2n+1} \right)^{n-1} \frac{1}{n} \cdot \\
 & \quad \int_0^1 \left[ 1 + \left( \frac{\chi-1}{J} \right)^2 \lambda^2 \right]^{n+1/2} d\lambda - 2S_R \left( \frac{n}{2n+1} \right)^m \left( 1 - \frac{1}{\chi^{2m-1}} \right) \\
 & \quad \left[ \frac{2(\chi-1)}{J} \right]^{m+1} \int_0^1 \left[ 1 + \left( \frac{\chi-1}{J} \right)^2 \lambda^2 \right]^{n+1/2} d\lambda \quad (48)
 \end{aligned}$$

where

$$S_R = \frac{\psi_o}{\eta_o} \dot{\gamma}_w^{1+m-n} \quad (49)$$

$$R_e = \frac{\rho h v_1}{\eta_w} = \frac{\rho h^2}{\eta_o} \left( \frac{n}{2n+1} \right) \dot{\gamma}_w^{2-n} \quad (50)$$

$$\dot{\gamma}_w = \frac{2n+1}{n} \frac{v_1}{h} \quad (51)$$

## RESULTS AND DISCUSSION

In order to calculate the die swell ratio ( $\chi$ ) versus shear rate ( $\dot{\gamma}$ ) or recoverable shear ( $S_R$ ) in Eq. (42) and Eq. (48), the viscosity versus shear rate data and the primary normal stress coefficient versus shear rate data were needed. Figure 5 plots the viscosities of PP and PS as functions of shear rate at 180°C, which were taken from experimental data of White and Roman.<sup>8</sup> PP was more viscous than PS at 180°C. Both polymers represented pseudoplastic behavior, the viscosity decreased with increasing shear rate. Figure 6 showed

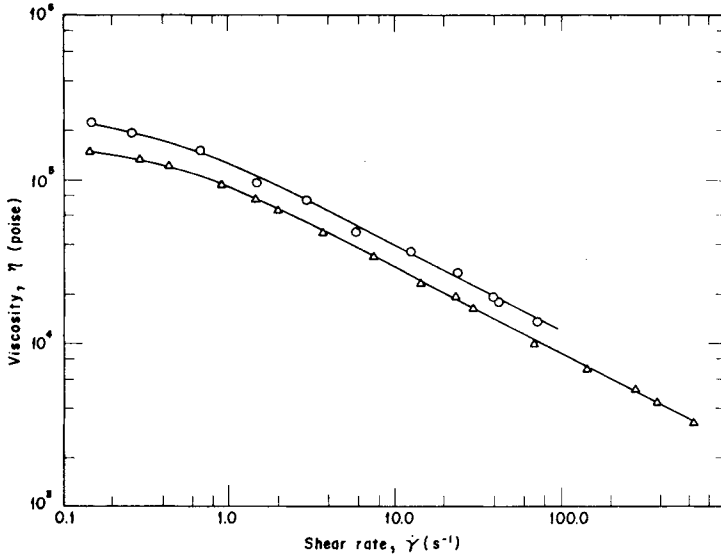


Fig. 5. Viscosity vs. shear rate for PP (○) and PS (Δ) at 180°C.

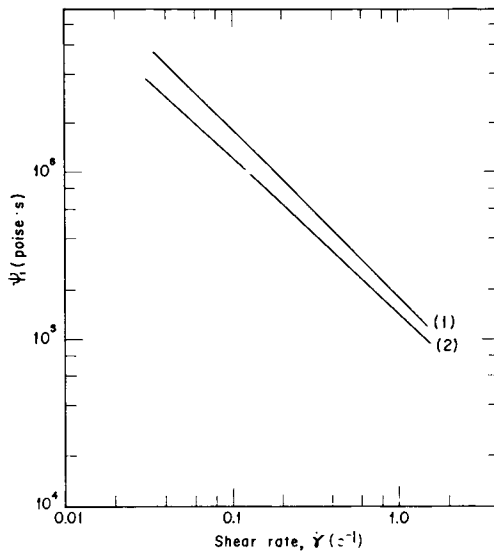


Fig. 6. Primary normal stress coefficient vs. shear rate for PP (1) and PS (2) at 180°C.

the data of primary normal stress coefficient versus shear rate for PP and PS at 180°C.<sup>8</sup> It seemed that the polymer with higher viscosity would have higher primary normal stress coefficient. And the primary normal stress coefficient decreased linearly in log-log scale with increasing shear rate. From the plots of Figures 5 and 6, all the constants in CEF equation (i.e.,  $\eta_0$ ,  $n$ ,  $\psi_0$  and  $m$ ) could be obtained by curve fitting. Table I lists these constants for PP and PS, which were used in calculating the die swell ratio in Eq. (42). Figures 7 and 8 plots the die swell ratio from capillary die versus shear rate at 180°C

TABLE I  
 Constants in CEF Equation, Obtained by Fitting Figures 5 and 6

	$\eta_0$	$n$	$\psi_0$	$m$
PP	$1.2 \times 10^5$	0.50	$1.75 \times 10^5$	-0.026
PS	$9.6 \times 10^4$	0.47	$1.35 \times 10^5$	0.040

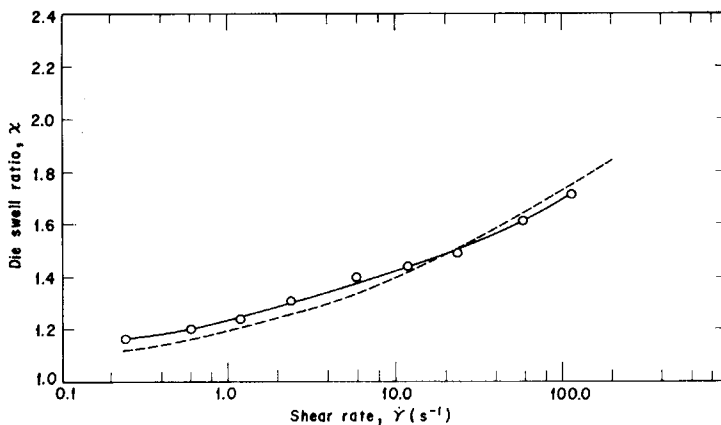


Fig. 7. Die swell ratio vs. shear rate for PP at 180°C. (—○—) Exp., (----) Eq. 42.

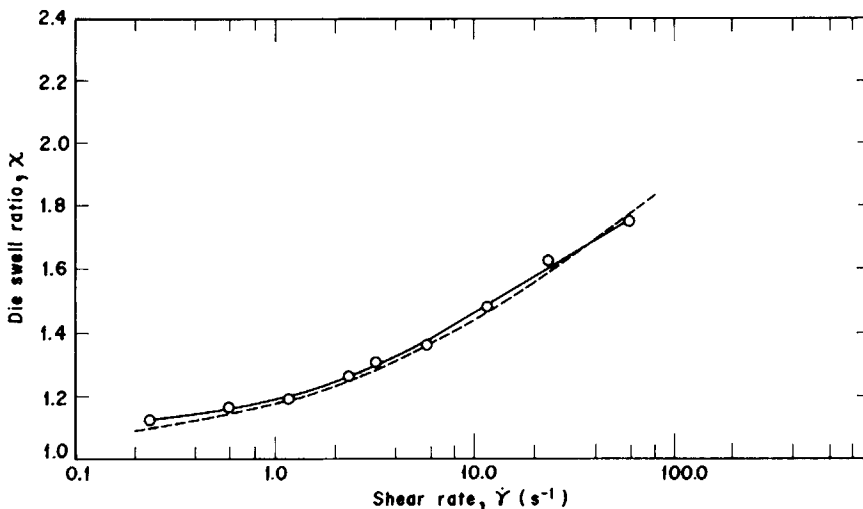


Fig. 8. Die swell ratio vs. shear rate for PS at 180°C. (—○—) Exp., (----) Eq. 42.

for PP and PS, respectively. Experimental results of White and Roman<sup>8</sup> were put in figures for comparison. Die swell ratio significantly increased with increasing shear rate due to the effects of normal stress and elastic recovery. The theoretical prediction conformed very well with the experimental data especially for PS. Since PP was a semicrystalline polymer, the crystallization kinetics would induce some error in the prediction of die swell. For example,

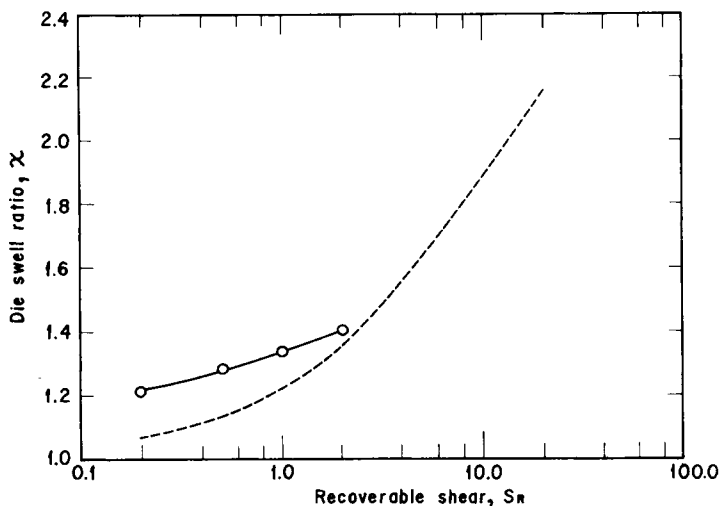


Fig. 9. Die swell ratio vs. recoverable shear for PP at 180°C. (—○—) Exp., (---) Eq. 42.

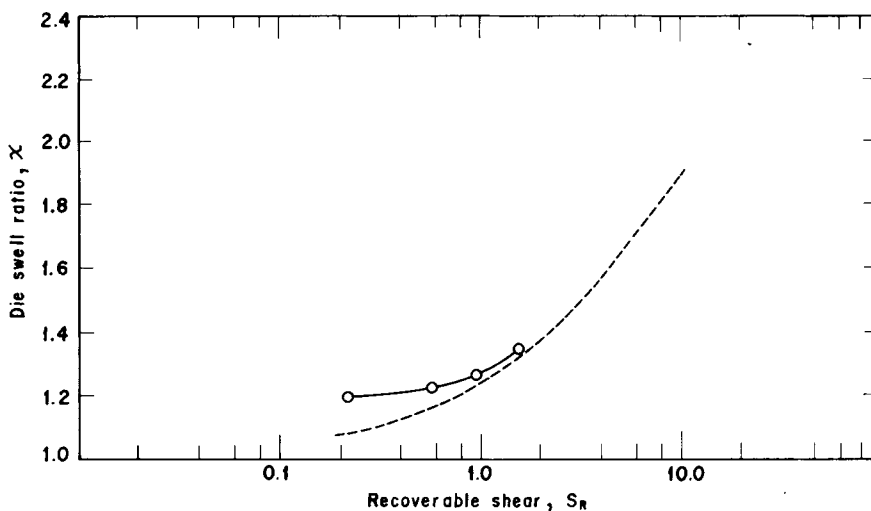


Fig. 10. Die swell ratio vs. recoverable shear to PS at 180°C. (—○—) Exp., (---) Eq. 42.

crystallization might change the molecular orientation, disturb the velocity profile, change the density and viscosity of fluid, and introduce internal stresses. Figures 9 and 10 show the relationship between die swell ratio from capillary die and recoverable shear for PP and PS, respectively. The experimental data were obtained from the cone-plate rheometer.<sup>8</sup> Due to instrumental limitation, higher recoverable shear data could not be obtained for comparison with the theoretical prediction.

Our equation underestimated the die swell ratio in the low recoverable shear region, but the error was within 10%. From the above results, we concluded that Eq. (42) could be used to predict the die swell of polymer fluids through capillary die. In a similar way, Eq. (48) could be expected to predict

the die swell of polymer fluids through a slit die. It would help us to know the effect of changing operating conditions on the die swell of polymer and would guide us to choose the proper conditions for the desired product.

### References

1. C. D. Han and K. U. Kim, *Polym. Eng. Sci.*, **11**, 395 (1971).
2. Y. Mori and K. Funatsu, *J. Appl. Polym. Sci.*, **20**, 209 (1973).
3. W. W. Graessley, S. D. Glasscock, and R. L. Crawley, *Trans. Soc. Rheol.*, **14**, 519 (1970).
4. C. D. Huang and J. L. White, *Polym. Eng. Sci.*, **9**, 609 (1979).
5. R. Racine and D. C. Bogue, *J. Rheol.*, **23**, 263 (1979).
6. A. B. Metzner, W. T. Houghton, R. A. Sailor, and J. L. White, *Trans. Soc. Rheol.*, **5**, 133 (1961).
7. R. I. Tanner, *J. Polym. Sci. A-2*, **8**, 2067 (1970).
8. J. L. White and J. F. Roman, *J. Appl. Polym. Sci.*, **20**, 1005 (1976); **21**, 869 (1977).
9. J. L. White and D. Huang, *Polym. Eng. Sci.*, **21**, 1101 (1981).
10. D. Huang and J. L. White, *Polym. Eng. Sci.*, **20**, 182 (1980).
11. R. I. Tanner, R. E. Nickell, and R. W. Bilger, *Comp. Meth. Appl. Mech. Eng.*, **6**, 155 (1975).
12. P. W. Chang, T. W. Patten, and B. A. Finlayson, *Comp. Fluids*, **7**, 267 (1979).

Received March 10, 1987

Accepted May 22, 1987